Proceedings of ASME 2018 Pressure Vessels and Piping Conference
PVP2018
July 15-20, 2018, Prague, Czech Republic

PVP2018-84103

A BASIS FOR APPLYING ELASTIC PERFECTLY-PLASTIC DESIGN METHODS TO CYCLIC SOFTENING MATERIALS

M. C. Messner
Argonne National Laboratory
Lemont, Illinois, USA

Yanli Wang
Oak Ridge National Laboratory
Oak Ridge, Tennessee, USA

R. I. Jetter
R. I. Jetter Consulting
Pebble Beach, California, USA

T.-L. Sham
Argonne National Laboratory
Lemont, Illinois, USA

ABSTRACT

Design approaches using elastic perfectly-plastic (EPP) analysis have recently been approved as Code Cases for the Section III, Division 5 design of high-temperature nuclear reactor components made from austenitic stainless steel. These methods bound the ratcheting strain and creep-fatigue damage accumulated over the life of a component with a simplified, elastic-perfectly plastic analysis using a special pseudo-yield stress – often not equal to the true material yield stress. The austenitic materials specified in the existing Code cases are cyclic-hardening for all allowable operating temperatures. However, other Section III, Division 5 materials, such as Grade 91 steel, are cyclic softening at expected advanced reactor operating temperatures. This work describes the extension of EPP methods to cyclic softening materials through the use of a postulated saturated material state and softening factors to be applied to the pseudo yield stress. We demonstrate the conservatism of the modified EPP method against a series of inelastic simulations of two bar tests, using a constitutive model that captures work and cyclic softening.

1 Introduction

Section III Code Cases N-861 and N-862 [1, 2] establish methods for evaluating structures against the Section III, Division 5 limits on strain accumulation and creep-fatigue damage using simplified elastic perfectly-plastic (EPP) analysis. The EPP procedures are designed to be simple and easy to execute compared to the base Code design by elastic analysis or design by inelastic analysis procedures. Numerous previous works demonstrate the advantages of the EPP methods and their applicability to a variety of design situations .

The current Code cases apply only to 304H and 316H austenitic stainless steel. These materials are cyclic hardening at all use temperatures allowed by the Code. However, other Code materials, like Grade 91 steel, are cyclic softening at elevated temperatures [8–10]. The EPP procedures have not been evaluated for use with softening materials. The deformation and damage bounds underlying the methods are based on standard material flow theory, which seems to preclude a cyclic softening response . As such, the procedures in the current Code cases may not be conservative for softening materials like Grade 91.

This work evaluates the applicability of the current EPP procedures by comparing the design lives calculated from the procedures to the results of a full inelastic analysis using a reference inelastic material model. The EPP calculations use consistent design data: yield stresses, isochronous curves, fatigue curves, rupture stresses, and interaction diagrams developed from simulated experiments using the reference inelastic material model. This ensures that the comparisons between the EPP methods and the inelastic simulations are consistent – differences between the response of the inelastic model and the average material response captured by the design data in the Code for a particular material

do not affect the comparison.

The results of this comparison show that the EPP method for creep-fatigue damage evaluation will apply to softening materials without requiring a modified database of material properties. The effects of cyclic softening are captured in the creep-fatigue interaction diagram. However, the Code Case procedure for the strain accumulation design limit, using isochronous curves derived from creep simulations on material without prior deformation history, does not produce conservative design lives for softening materials. The design data underlying this EPP method – temperature dependent yield stresses and isochronous curves – do not account for material softening. As such, this work proposes modifying the Code isochronous stress/strain curves to account for prior cyclic deformation and using this modified material property database in the EPP strain accumulation method for softening materials. The simulations described here demonstrate that, after applying modifications to the underlying material properties, the EPP method conservatively bounds strain accumulation in cyclic softening materials.

Section 2 describes the reference inelastic material model, the development of the consistent design data from simulated experiments, and the example structural component used in this study. Sections 3 and 4 compare the EPP procedures to the inelastic model results and propose modifications to account for softening, where required. The final section summarizes the results of the work.

2 Reference inelastic simulations

2.1 Material model

This work addresses softening in the EPP design methods by comparing the design calculations to a reference inelastic material model. The inelastic model should describe a realistic material response, in particular a realistic treatment of cyclic softening, but need not exactly correspond to any real material. The life of a structure, as simulated with the inelastic model, is taken as the ground truth. This baseline life is compared to EPP design calculations using consistent design curves generated from simulated experiments using the inelastic model. The EPP methods should be conservative; that is the EPP design life should be less than the actual simulated life of the structure.

The model has two parts: a model for deformation and creep damage combined with a damage model for capture cyclic fatigue damage. The reference inelastic deformation model is a generalized unified viscoplastic Chaboche model with two backstresses, including the static recovery terms. The model includes isotropic softening using a Voce formulation with a negative saturation stress to capture cyclic softening. This softening term also represents the transition from primary to tertiary creep, so that the base model for material deformation produces realistic creep curves and creep rupture lives. Parameters are temperature dependent and the model is applicable from room temperature to 650° C. The deformation part of the model is loosely based on a model developed by the authors and others for Grade 91 steel.

A damage model, representing fatigue damage, supplements this inelastic deformation model. The model is ad hoc, invented by the authors for this particular application. It assumes damage is proportional to the total effective strain rate and so can handle both low cycle and high cycle fatigue. The model includes a delay term so that damage does not accumulate uniformly over some prescribed strain controlled cyclic life. Instead, damage first accumulates slowly and later quickly accelerates to produce a realistic strain-controlled cyclic history.

The EPP methods and the ASME Section III, Division 5 Code in general rely on five kinds of design information when evaluating a structure's ratcheting and creep-fatigue lives: yield stress tables, isochronous stress-strain curves, fatigue curves, creep rupture stresses, and a creep-fatigue interaction diagram, i.e. the D-diagram. These design curves are generated from experimental data. Here, we generate these standard design curves using simulated experiments with the reference inelastic model. This allows a consistent comparison between the inelastic model and the EPP approaches even if the inelastic model does not perfectly represent the response of Grade 91.

A yield stress table for the inelastic model was created by simulating uniaxial tension tests at different temperatures and the ASTM E21 [19] standard strain rate of $0.005\,\mathrm{mm/mm/min}$. For each simulated tension curve the yield stress was computed with a 0.2% offset and tabulated as a function of temperature.

Figure 1 shows examples of isochronous curves generated from simulated creep tests using the inelastic model. The figure compares these generated curves to the Code Grade 91 isochronous curves. This example is at 550° C but similar curves were generated for temperatures between 300° C and 650° C – below this range the model predicts negligible creep. The model agrees well with the Code curves, implying the inelastic model is reasonably representing creep deformation.

Similar simulated creep tests were used to generate rupture life data at different temperatures. Failure in these simulations is defined as the point where the numerical time stepping diverged as the model strain rate rapidly increased, indicating the onset of material failure. Figure 2 plots this simulated data in terms of the Larson-Miller [20] parameter

$$LM = T\left(\log t + C\right). \tag{1}$$

A linear trend line fits the data to the rupture stress in log space. An optimal value of C was included in the regression, with the result being $C = 30.4$. Per the ASME standard procedure this linear trend line was adjusted downwards to a 90% confidence lower bound on the data. This lower bound is used as the rupture life curve in the subsequent EPP calculations. The model rupture lives agree well with the Grade 91 Code data.

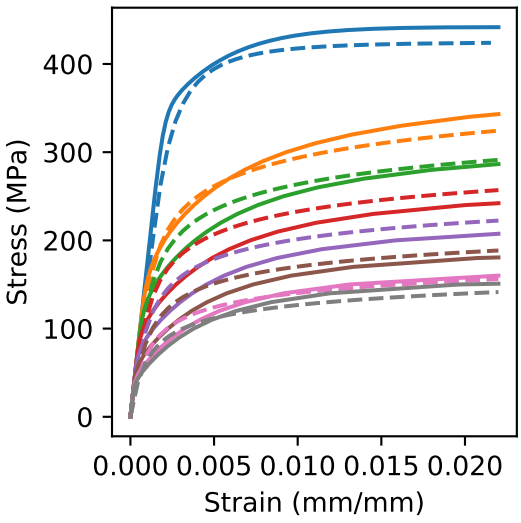

FIGURE 1. Isochronous curves for the reference inelastic material model generated by simulating a series of creep tests and compared to the Code isochronous curves for Grade 91 at 550° C. The solid lines are the simulated curves, the dashed lines are the Code curves. The curves in order from top to bottom are the hot tensile curve and then isochronous curves for 1 hour life, 10 hours life, 100 hours life, 1,000 hours life, 10,000 hours life, 100,000 hours life, and 300,000 hours life.

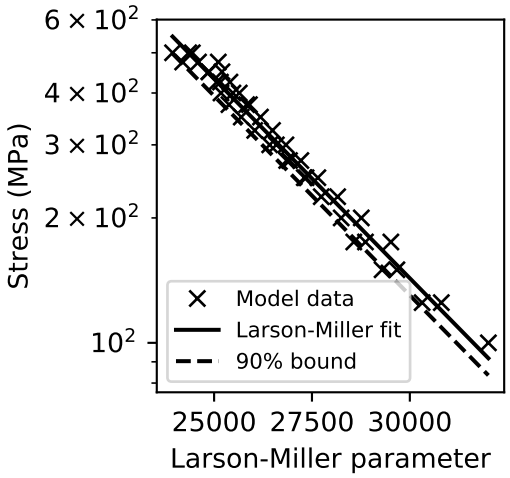

FIGURE 2. Simulated rupture life data plotted on a Larson-Miller diagram. The figure shows both the raw data and the 90% lower bound used as the design curve.

Note there is scatter in the creep rupture simulations when compared to the Larson-Miller trend line. The model is deterministic, however the numerical time stepping scheme means that the model predictions will randomly undershoot the true, analytic rupture life of the model obtained through an exact integration of the constitutive equations. In practice, the equations are integrated numerically with a time stepping scheme that advances the model from time t_n to $t_n + \Delta t$. In the creep regime the time step, Δt, is quite large to reduce the number of load steps required for the simulation. At the end of the simulation the final load step will diverge – the numerical integration scheme will fail. This means the model failed somewhere in between t_n to $t_n + \Delta t$. The results here take the rupture time to be the last complete time step t_n. This introduces an error of at most Δt into the computed rupture lives.

A series of simulated fatigue tests were used to develop a fatigue life relation for the reference model. These simulated fatigue tests are strain-controlled, fully reversed loading for various strain ranges at a strain rate of $4 \times 10^{-3}\,\mathrm{s}^{-1}$ and at 540° C, corresponding to the Code fatigue curve for Grade 91. In these simulations failure is defined as the number of cycles at which the simulated maximum cycle stress falls below 25% of the maximum stress over the first cycle. The damage model used to represent fatigue damage here is temperature independent and so the resulting consistent fatigue curves will likewise be temperature independent. Figure 3 shows results from an example simulated fatigue tests. These plots show the maximum stress and minimum stress over a load cycle, plotted as a function of cycle count. The figure shows results for the material model with the damage term on and the model with the damage term off. The shape of these curves, with the damage model on, is reasonable for Grade 91. Typically, under cyclic load Grade 91 will soften, appear to be approaching some saturated softened flow stress, but then the stresses will abruptly fall off as damage develops in the material. Figure 4 shows the simulated fatigue data and the Code fatigue curve for Grade 91. The model and the Code data for Grade 91 deliberately do not agree – the model develops fatigue damage much quicker than the actual material. This is intentional to reduce the number of cycles to failure to lessen the simulation time. Additionally, Fig. 4 shows shifted curves from the model simulated fatigue data, one curve representing a reduction by a factor of two on the strain range and another representing a reduction of 20 on the fatigue life. The lower of these curves is used as the consistent model design fatigue curve. This method is the ASME procedure for generating a design fatigue curve from raw data.

Finally, Fig. 5 plots data from simulated creep-fatigue experiments. The simulated experiments are of fully-reversed strain controlled cyclic deformation at various strain ranges with holds of various times on the tensile stress side of the cycle. These simulated experiments were repeated at various temperatures. The simulations run until the simulated maximum cycle stress falls below 25% of the initial maximum stress, which is

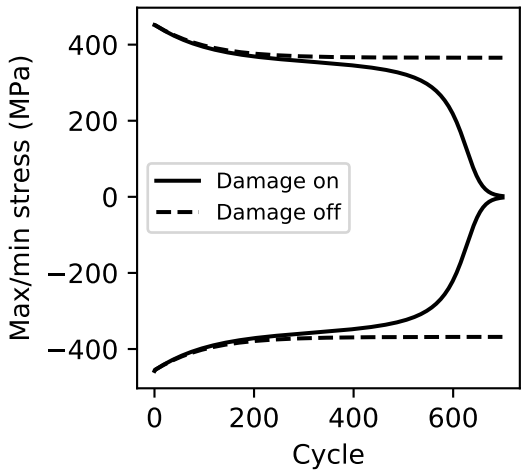

FIGURE 3. Example simulations of fatigue tests at $T = 540^{\circ}$C with a strain range of 1%. The figure plots the simulated maximum and minimum stress per cycle. The results shown with solid lines include the fatigue damage terms; the results shown with dashed lines are from simulations with the damage term turned off.

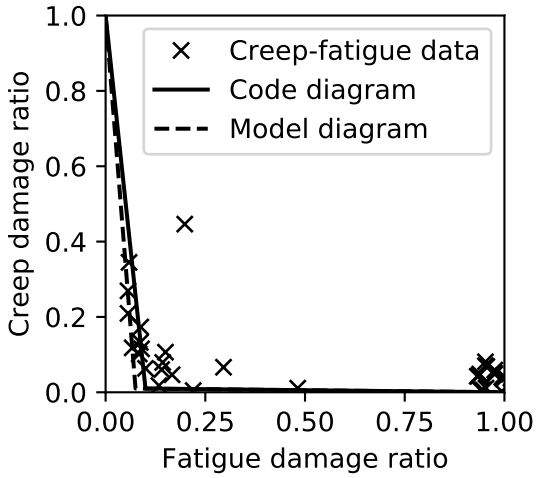

FIGURE 5. Results of simulated creep-fatigue tests plotted on a D-diagram. The figure also shows the interaction curve used in the consistent EPP calculations and the Code curve for Grade 91. For this example, the D-diagram was fit to closer to the minimum, rather than the average, of the simulated data.

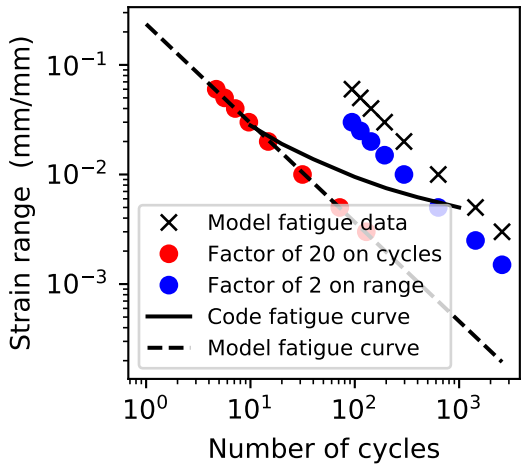

FIGURE 4. Model fatigue curve compared to the ASME fatigue curve for Grade 91. The figure shows both the raw model data and the two curves used to set the design fatigue curve according to the ASME procedure.

defined as failure. The data for each experiment are plotted as points on a D-diagram. The number of cycles to failure is converted to a fatigue damage index by dividing by the number of cycles to failure from the design fatigue curve described in the previous paragraph, stripped of the safety factors. The stress relaxation during the hold is converted to a creep damage index using the Section III, Division 5 procedure, referencing the consistent model rupture life curve described above, stripped of the safety factors. The resulting points describe creep-fatigue damage interaction. The figure shows an interaction curve drawn to match the model simulations along with the Code interaction curve for Grade 91. The curves are similar, but the model curve is shifted slightly left to better match the simulated creep-fatigue experiments. Both the simulated material and Grade 91 have severe creep-fatigue interaction.

The apparent scatter in the creep-fatigue simulation data is partly due to the time stepping scheme discussed above in reference to the simulated creep rupture lives. However, it mostly occurs because the inelastic model does not posit a bilinear interaction diagram – that is, there is no reason why an exact integration of the constitutive equations should predict a bilinear creep-fatigue interaction. The scatter in the model data then reflects randomly selected creep-fatigue loading conditions.

2.2 Example geometry

Figure 6 shows the example structure used in this work. This is a two bar structure under a combination of primary and secondary load. The primary load is applied via a force shared between the two bars. Changing the temperatures of the two bars induces the secondary stress. The two bar system is interpreted as representing fibers through the thickness of a vessel under pressure loading and a through wall thermal gradient. The tempera-

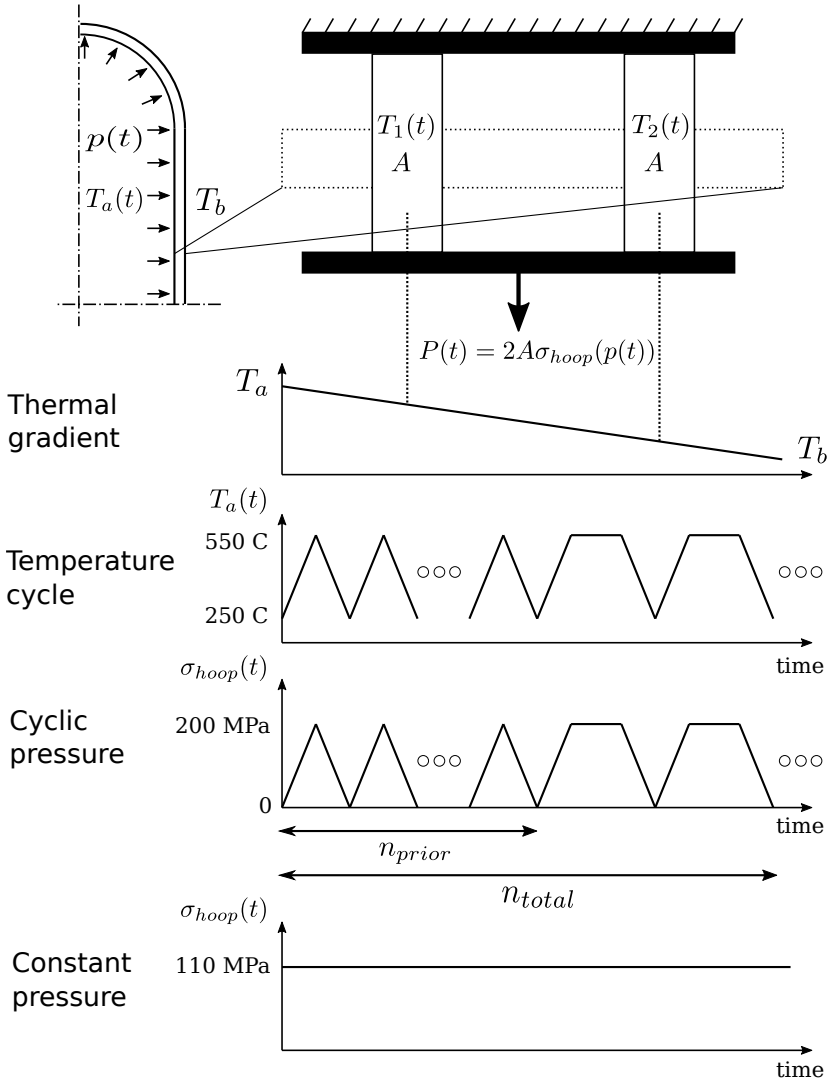

FIGURE 6. Two bar system used as an example component in this work. The two bars are taken to represent two fibers of a through-wall cross section of a thin walled pressure vessel under a combination of a pressure load and a linear temperature gradient. The area and length of the bars factor out of the equations describing the system and so were set arbitrarily. The vessel thickness affects the calculation only in that it converts the pressure in the vessel to a hoop stress applied to the two bar system. Therefore, we just apply the load in terms of the hoop stress σ_{hoop} directly. This work considers two loading histories: one where primary stress is constant and another where the primary stress cycles. The temperatures of the two bars vary in both load histories.

ture of each bar is set by its location through the wall thickness. The figure describes the two load cases considered here: a constant primary load and an alternating primary load. Both load cases have an alternating temperature profile. The temperature cycle keeps a fixed outer wall temperature of 250° C. The inner wall temperature alternates between 250° C and 550° C. For the first n_{prior} cycles, called the "pre-loading" or "pre-fatigue" below, the heating/cooling rate of the inner wall is $\dot{T} = 100^\circ\,\mathrm{C/hour}$ and there is no hold at temperature. For the remaining cycles the heating/cooling rate remains the same but now the loading maintains the hot temperature for 100 hours.

For the cyclic primary load case the hoop stress stays in phase with the temperature. For the first n_{prior} cycles the load alternates between 0 and 200 MPa at a loading rate set to keep the mechanical load in-phase with the temperature loading. For the remaining cycles the stress alternates at the same rate but now with a hold of 100 hours at the maximum stress. In the constant primary load case the hoop stress on the system remains constant

at 110 MPa.

3 EPP strain limits

3.1 EPP procedure using standard isochronous curves

This section, addressing the ratcheting strain limits, uses the constant primary load case. Furthermore, the reference inelastic simulations in this section do not use the fatigue damage model. This is to ensure that the simulations do not predict creep-fatigue failure before the structure reaches the ratcheting limits.

The strain accumulation criteria in Section III, Division 5 define failure as any of the following occurring: a) the average inelastic strain through a section exceeds 1%, b) the linearized strains at the surface exceed 2%, or c) the maximum strain exceeds 5%. For a two bar problem, interpreted as fibers through the thickness of a vessel, criteria a) and b) are equivalent and criteria c) will never occur before a) and b). Therefore, determining the ratcheting life of the structure involves simulating repeated load cycles, as described in Fig. 6, until the average strain in the two bars reaches 1%. The time required to reach this condition is the life of the simulated system, as defined by the Code. Figure 7 plots this life as a function of the number of pre-cycles, n_{prior}. The pre-cycles are pure fatigue, i.e. there is no hold at a constant stress or strain. Their purpose is to apply some cyclic softening to the system before imposing the more standard combination of alternating thermal load and a hold at fixed temperature. If cyclic softening affects the structure's life or the conservatism of EPP design procedures, using standard isochronous curves, that effect should become more significant as the number of pre-cycles, and hence the amount of prior cyclic softening, increases.

A corresponding EPP strain limits calculation, using the Code Case developed for the cyclic hardening austenitic stainless steels, requires defining a composite cycle. This is a single load cycle encompassing all the relevant features of all the design load cycles for a particular component. Because the EPP analysis is rate independent holds can be neglected when defining the composite cycle. In the case of this simple structure defining the composite load cycle is straightforward. The stress is constant and the temperature follows the alternating load cycle defined in Fig. 6 without the hold. Note that this composite load cycle captures both the pre-cycles and the standard load cycle and so, for the base the Code Case, there will be only one EPP design life for the structure regardless of the number of pre-cycles.

The EPP strain limits Code Case applies EPP analysis using a psuedo yield stress defined in terms of the material yield stress, the isochronous curves, a target strain, and some trial design life t'_{life}. The calculations here use the yield stress table and isochronous curves developed from the simulated experiments described in the previous section. Note these data correspond to the Code data derived from experiments on material in the as-received condition. That is, the data do not account for cyclic softening. Tthe comparison between the inelastic model and the EPP calculation is consistent – the underlying design data reflects the properties of the reference material defined by the inelastic model. Figure 7 plots this EPP design life. For this composite cycle, using the base Code Case procedure to define the pseudoyield stress, the structure deforms elastically for any design life up to 300,000 hours. Therefore, the two bar system shakes down, the accumulated inelastic strain is zero, and the system passes the EPP check. The base EPP design life for the system is then greater than 300,000 hours. Clearly the EPP procedure, using a database reflecting the properties of material in the as-received state, is non-conservative for this particular material model and two bar system – the EPP design life exceeds the reference life computed via the inelastic model. Note that the degree of non-conservatism increases as the number of pre-cycles increases: the life computed by inelastic analysis decreases but the EPP design life remains the same. This suggests that the defect in the EPP procedure relates to cyclic softening.

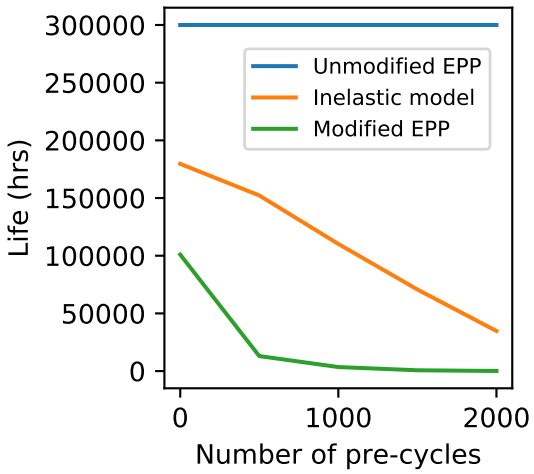

FIGURE 7. Comparison between the EPP and the simulated ratcheting design lives for the two bar structure. The figure shows the design life as a function of the number of pre-cycles. The plot shows design lives as calculated from two EPP procedures: the unmodified Code Case for austenitic stainless steel and the modified approach proposed here to account for cyclic softening. The unmodified procedure actually produces a design life greater than the indicated 300,000 hours – 300,000 hours is the longest life isochronous curve generated for this study.

3.2 Accounting for cyclic softening in the isochronous curves

The EPP N-861 Code Case applies only to 304H and 316H austenitic stainless steel. These materials are cyclic hardening whereas the reference material here is cyclic softening. This is

a significant difference. The ratcheting Code Case relies on the isochronous curves to bound the accumulated creep deformation. With a softening material fatigue pre-cycling decreases the material flow stress, increasing the amount of subsequent creep deformation.

This manifests in the isochronous curves. Conceptually, a set of softened isochronous curves could be developed where the material was first pre-cycled under some specified conditions before creep deformation. These softened creep curves could then be collated into softened isochronous curves. This process can easily be done via numerical simulation. Figure 8 shows an example set of softened and unsoftened isochronous curves for the reference material at 550° C. The prior cyclic softening increases the subsequent creep deformation, lowering the resulting isochronous curves.

Fundamentally, this softening explains why the Code Case EPP procedure is non-conservative for cyclic softening materials – the base isochronous curves, which do not account for softening, underestimate the creep deformation. One way to apply the EPP procedure to softening materials would be to use softened isochronous curves. Define the softened isochronous curve as:

$$\sigma_{icc}\left(\varepsilon, T, t_{life}, \Delta\varepsilon, N\right). \tag{2}$$

That is, the isochronous curve is a function of strain, temperature, and design life, as with the standard curves in the Code, but also a function of the strain range $\Delta\varepsilon$ and number of cycles N. It would be difficult or impossible to determine these kinds of isochronous curves experimentally but they can easily be simulated using the reference material model. A similar function can be defined for the softened material yield stress – the initial flow stress after N cycles of strain controlled loading with a strain range of $\Delta\varepsilon$.

Figure 7 shows the design life as calculated with the EPP procedure using the softened isochronous curves. The modified procedure is the same as the Code Case procedure except instead of the standard yield stress and isochronous curves the pseudo yield stress is defined using the softened yield stress and softened isochronous curves. The relevant strain range can be determined from the full inelastic analysis – approximately 0.4% – and the number of cycles can be determined from the trial life t'_{life}. The plot shows that this modification produces conservative design lives – now the modified EPP design lives are less than the corresponding lives obtained through full inelastic simulation. The design life from the modified procedure is now a function of the number of pre-cycles: for a fixed trial life t'_{life} increasing the number of pre-cycles increases the total number of cycles because the pre-cycle period is much smaller than the full cycle period. The modification affects the EPP life without any pre-cycling because cyclic softening occurs even during the full design cycles. This softening during the main cycles is accounted for in the modified procedure but not in the base procedure.

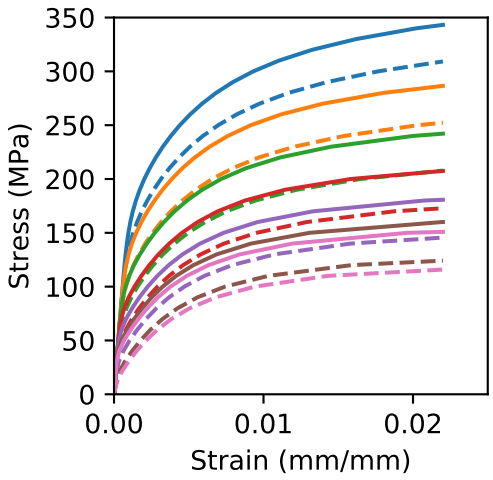

FIGURE 8. Example softened isochronous curves at 550° C, as simulated by the reference inelastic material model. In order from top to the bottom the curves are for 1 hour life, 10 hours life, 100 hours life, 1,000 hours life, 10,000 hours life and 100,000 hours life. The solid lines show the curves without prior cyclic softening, i.e. the creep simulations begin with virgin material without any prior history. The dashed lines show corresponding isochronous curves generated from simulated creep tests starting after 1000 cycles of fully reversed strain controlled deformation with a strain range of 0.4%.

The proposed modification allows the conservative use of EPP methods for checking ratcheting strain accumulation for cyclic softening materials. However, the full version described here would not be practical to implement in the Code for several reasons. The first is that gathering the experimental data to develop softened isochronous curves would be challenging. As described above, the softened curves are a function of temperature, life, strain range, and number of cycles. Therefore, a large series of creep test data at different stresses and temperatures and with different amounts of prior fatigue would be required. Developing this experimental database would be time consuming and expensive. Even assuming the existence of the required experimental data the softened isochronous curves would be difficult to tabulate in the Code as they would be a function of five variables. Additionally, the full modified procedure would complicate the Code Case rules as they would require determining the actual number of cycles and the characteristic strain range of each cycle that a structure experiences in its lifetime. Determining the strain range would be a substantial challenge as a self-contained procedure could not rely on full inelastic analysis as was used here. Finally, rules would need to be developed to accumulate softening from cycles with different strain ranges.

An alternative procedure relying on a saturated softened material state would avoid most of these difficulties. Figure 3 il-

lustrates this idea. Without the damage model the cyclic softening curves simulated with the inelastic material model eventually reach a saturated state – the material flow stress stops decreasing. With the damage model turned on the material never saturates because the cyclic softening blends into softening caused by damage accumulation. However, one could hypothesize a saturated material state if damage did not occur. This saturated state could be measured experimentally by ignoring the later part of a cyclic softening curve attributed to damage and, if necessary, extrapolating the early data out to a saturated state.

The EPP procedure could use the isochronous curves based on this saturated material state. The necessary experiments would be a series of creep tests carried out after a large amount of prior fatigue – enough to saturate or nearly saturate the cyclic softening without developing damage. By referencing these saturated, softened curves the EPP procedure could avoid the challenge of determining a strain range or an actual cycle count but still expect to bound the accumulated ratcheting deformation. The procedure could be further simplified by tabulating softening factors as a function of the design life and temperature. This softening factors would be the ratio between the value of the softened isochronous curve and the unsoftened curve for some value of target strain. As the amount of softening is approximately constant with increasing strain these factors could be developed only for a single value of target strain, likely 1%, and applied to any value of target strain. This modified procedure would be straightforward to apply, not substantially more complicated than the existing procedure for 304H and 316H. However, this simplification may come at the expensive of overconservatism.

One objection could be that the simplified modified procedure may underestimate the amount of accumulated deformation if the structure develops substantial creep-fatigue damage, causing additional softening. However, the creep-fatigue provisions of the Code are designed to prevent such an accumulation of damage. Therefore, even though the ratcheting strain check may be non-conservative in this deformation regime the overall Code would remain conservative, as such a structure would fail the creep-fatigue design check.

A technical report from Argonne National Laboratory describes the process of establishing softening factors for Grade 91 in greater detail, referencing both experimental and modeling results [21].

4 EPP creep-fatigue

A similar process can be used to asses the effect of cyclic softening on the existing Code Case EPP procedures for creep-fatigue damage. The same structure and reference inelastic model are used to simulate a base component life as a function of the number of pre-cycles. These simulations now include the fatigue damage model and use the alternating primary stress load cycle. Failure is defined as when the flow stress in one of the bars falls below 25% of the initial flow stress. Figure 9 plots the simulated design life as a function of the number of pre-cycles.

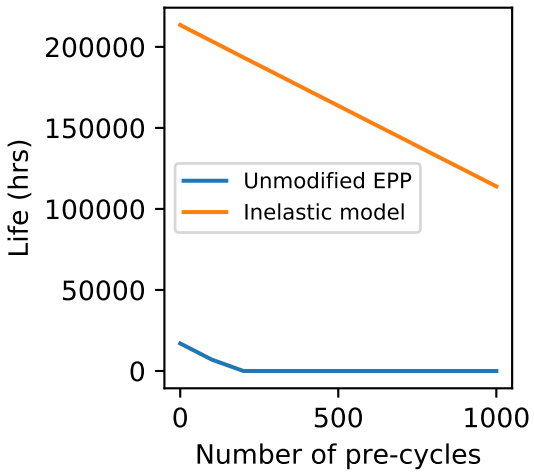

FIGURE 9. Plot comparing the simulated life of the two bar structure with cyclic primary load to the corresponding EPP design life, using the base Code Case procedure. The figure plots design life as a function of pre-cycles.

As before, defining an appropriate composite load cycle for the corresponding EPP design check is trivial – it is again just the cycle without any hold and applies to both the pre-cycles and the main load cycles. The Code Case EPP procedure for creep-fatigue uses a pseudo yield stress defined by referencing the material rupture stress. The procedure then computes creep-fatigue damage using material fatigue curves and interaction diagram. Figure 9 plots the EPP design life of the two bar structure, again as a function of the number of pre-cycles. These EPP calculations use the consistent design data generated in Section 2. In contrast to the strain limits procedure the unmodified EPP creep-fatigue method, developed for cyclic hardening materials, produces conservative design lives. The EPP design life goes to zero at around 250 cycles of pre-fatigue. This is because the EPP procedure allows only about 250 cycles of pure fatigue loading.

The EPP procedure for creep-fatigue does not require modification to account for softening because the creep-fatigue interaction diagram already accounts for the softening effect. This diagram is created by plotting the results of creep-fatigue experiments on a normalized scale. This data includes the effect of cyclic softening, which occurs over the course of the experiments. Softening materials will tend to have severe creep-fatigue interaction leading to very restrictive D-diagrams. The D-diagram for the reference inelastic material model used here and the diagram for Grade 91 in the Code reflect this severe interaction.

The EPP procedure is very conservative even for zero pre-

fatigue cycles. This reflects the conservatism in the ASME Code fatigue curves and in the EPP method. The large reductions applied to the Code curves are intended to account for sample-to-sample variability and environmental effects, neither of which affect the reference inelastic model. Additionally, the current EPP creep-fatigue procedure is highly conservative because it requires establishing elastic shakedown which severely limits the maximum allowable cyclic load.

5 Conclusions

This work assess the effect of cyclic softening on the EPP design procedure defined by Code Cases N-861 and N-862 [1,2]. These Code Cases only apply to 304H and 316H stainless steel, both of which are cyclic hardening materials, and so the purpose of this work is to develop a basis for applying the EPP procedures to softening material and to describe any changes needed to the underlying material database. The EPP procedure for evaluating creep-fatigue damage can be conservatively applied to softening materials using the existing Code data because the interaction Code diagram already accounts for the effects of cyclic softening. However, the EPP procedure for ratcheting strain limits will require the use of a modified database accounting for prior cyclic softening. The Code isochronous curves are developed from test results on virgin, unsoftened material. Prior cyclic softening tends to increase the amount of subsequent creep deformation. The current EPP procedure, referencing the Section III, Division 5 isochronous curves, does not capture the creep acceleration caused by cyclic softening. Conceptually, the EPP procedure should instead reference the softened material yield stress and isochronous curves, developed as functions of strain range and number of cycles. However, such a procedure will be difficult to implement. Therefore, this work recommends a simplified approach based on a saturated, softened material state.

ACKNOWLEDGMENT

The research was sponsored by the U.S. Department of Energy, under Contract No. DE-AC02-06CH11357 with Argonne National Laboratory, managed and operated by UChicago Argonne LLC, and under contract DE-AC05-00OR22725 with Oak Ridge National Laboratory, managed and operated by UT-Battelle LLC. Programmatic direction was provided by the Office of Nuclear Energy.

COPYRIGHT NOTICE

REFERENCES

[1] American Society of Mechanical Engineers, 2015. "Case N-861: Satisfaction of Strain Limits for Division 5 Class A Components at Elevated Temperature Service Using Elastic-Perfectly Plastic Analysis". In *ASME Boiler and Pressure Vessel Code, Nuclear Component Code Cases*.

[2] American Society of Mechanical Engineers, 2015. "Case N-862: Calculation of Creep-Fatigue for Division 5 Class A Components at Elevated Temperature Service Using Elastic-Perfectly Plastic Analysis". In *ASME Boiler and Pressure Vessel Code, Nuclear Component Code Cases*.

[3] Carter, P., Jetter, R. I., and Sham, T.-L., 2012. "Application of shakedown analysis to evaluation of creep-fatigue limits". In Proceedings of the ASME 2012, pp. 1–10.

[4] Carter, P., Jetter, R. I., and Sham, T.-L., 2014. "Verification of elastic-perfectly plastic methods for evaluation of strain limits - analytical comparisons". In Proceedings of the ASME 2014 Pressure Vessels & Piping Conference, pp. 1–8.

[5] Hollinger, G., Pease, D., Carter, P., Jetter, R. I., and Sham, T.-L., 2014. "Verification of elastic-perfectly plastic methods for evaluation of strain limits - demonstration example problem". In Proceedings of the ASME 2014 Pressure Vessels & Piping Conference, pp. 1–16.

[6] Sham, T.-L., Jetter, R. I., and Wang, Y., 2016. "Elevated temperature cyclic service evaluation based on elastic-perfectly plastic analysis and integrated creep-fatigue damage". In Proceedings of the ASME 2016 Pressure Vessels and Piping Conference, pp. 1–10.

[7] Messner, M., Sham, T.-L., and Jetter, R., 2017. "Verification of the epp code case for strain limits evaluations by inelastic analysis method". In Proceedings of the 2017 ASME Pressure Vessel and Piping Conference, Vol. 1B-2017.

[8] Shankar, V., Valsan, M., Rao, K. B. S., Kannan, R., Mannan, S. L., and Pathak, S. D., 2006. "Low cycle fatigue behavior and microstructural evolution of modified 9Cr-1Mo ferritic steel". *Materials Science and Engineering A,* **437**(2), pp. 413–422.

[9] Zhang, K., and Aktaa, J., 2016. "Characterization and modeling of the ratcheting behavior of the ferritic-martensitic

steel P91". *Journal of Nuclear Materials,* **472**, pp. 227–239.

[10] Fournier, B., Sauzay, M., and Pineau, A., 2011. "Micromechanical model of the high temperature cyclic behavior of 9-12%Cr martensitic steels". *International Journal of Plasticity,* **27**(11), pp. 1803–1816.

[11] Carter, P., 1985. "Bounding theorems for creep-plasticity". *International Journal of Solids and Structures,* **21**(6), pp. 527–543.

[12] Carter, P., 2005. "Analysis of cyclic creep and rupture. Part 1: Bounding theorems and cyclic reference stresses". *International Journal of Pressure Vessels and Piping,* **82**(1), pp. 15–26.

[13] Carter, P., 2005. "Analysis of cyclic creep and rupture. Part 2: Calculation of cyclic reference stresses and ratcheting interaction diagrams". *International Journal of Pressure Vessels and Piping,* **82**(1), pp. 27–33.

[14] Ainsworth, R. A., 1979. "Bounding solutions for creeping structures subjected to load variations above the shakedown limit". *International Journal of Solids and Structures,* **15**(12), pp. 981–986.

[15] Ainsworth, R. A., 1979. "Appplication of bounds for creeping structures subjected to load variations above the shakedown limit". *International Journal of Solids and Structures,* **13**, pp. 981–993.

[16] Chaboche, J. L., and Cailletaud, G., 1986. "On the calculation of structures in cyclic plasticity or viscoplasticity". *Computers and Structures,* **23**(1), pp. 23–31.

[17] Chaboche, J., 1989. "Constitutive equations for cyclic plasticty and cyclic viscoplasticity". *International Journal of Plasticity,* **5**, pp. 247–302.

[18] Chaboche, J. L., 1991. "On some modifications of kinematic hardening to improve the description of ratchetting effects". *International Journal of Plasticity,* **7**(7), pp. 661–678.

[19] ASTM International, 2009. E 21-09: Standard Test Methods for Elevated Temperature Tension Tests of Metallic Materials.

[20] Larson, F. R., and Miller, J., 1952. "A time-temperature relationship for rupture and creep stresses". *Transactions of the ASME,* **74**, pp. 765–771.

[21] Messner, M. C., and Sham, T.-L., 2017. FY17 Status Report on the Initial EPP Finite Element Analysis of Grade 91 Steel. Tech. rep., Argonne National Laboratory, ANL-ART-94 136949.